ANTIOXIDANTS & REDOX SIGNALING
Volume 22, Number 18, 2015

DOI: 10.1089/ars.2014.6078

Discoveries

FORUM ORIGINAL RESEARCH COMMUNICATION

Isolevuglandin-Type Lipid Aldehydes Induce the Inflammatory Response of Macrophages by Modifying Phosphatidylethanolamines and Activating the Receptor for Advanced Glycation Endproducts

Lilu Guo,[1] Zhongyi Chen,[1] Venkataraman Amarnath,[2] Patricia G. Yancey,[3] Brian J. Van Lenten,[4] Justin R. Savage,[5] Sergio Fazio,[6] MacRae F. Linton,[3,7] and Sean S. Davies[1,7,8]

Abstract

Aims: Increased lipid peroxidation occurs in many conditions associated with inflammation. Because lipid peroxidation produces lipid aldehydes that can induce inflammatory responses through unknown mechanisms, elucidating these mechanisms may lead to development of better treatments for inflammatory diseases. We recently demonstrated that exposure of cultured cells to lipid aldehydes such as isolevuglandins (IsoLG) results in the modification of phosphatidylethanolamine (PE). We therefore sought to determine (i) whether PE modification by isolevuglandins (IsoLG-PE) occurred *in vivo*, (ii) whether IsoLG-PE stimulated the inflammatory responses of macrophages, and (iii) the identity of receptors mediating the inflammatory effects of IsoLG-PE. ***Results:*** IsoLG-PE levels were elevated in plasma of patients with familial hypercholesterolemia and in the livers of mice fed a high-fat diet to induce obesity and hepatosteatosis. IsoLG-PE potently stimulated nuclear factor kappa B (NFκB) activation and expression of inflammatory cytokines in macrophages. The effects of IsoLG-PE were blocked by the soluble form of the receptor for advanced glycation endproducts (sRAGE) and by RAGE antagonists. Furthermore, macrophages derived from the bone marrow of *Ager* null mice failed to express inflammatory cytokines in response to IsoLG-PE to the same extent as macrophages from wild-type mice. ***Innovation:*** These studies are the first to identify IsoLG-PE as a mediator of macrophage activation and a specific receptor, RAGE, which mediates its biological effects. ***Conclusion:*** PE modification by IsoLG forms RAGE ligands that activate macrophages, so that the increased IsoLG-PE generated by high circulating cholesterol levels or high-fat diet may play a role in the inflammation associated with these conditions. *Antioxid. Redox Signal.* 22, 1633–1645.

Introduction

PEROXIDATION OF POLYUNSATURATED fatty acids *in vivo* has long been known to generate reactive lipid aldehydes, but much remains unknown about the biological importance of these reactive lipid aldehydes. Isolevuglandins (IsoLGs) are a family of eight highly reactive gamma-ketoaldehyde regioisomers generated by the peroxidation of arachidonic acid (8, 59). IsoLGs differ from α,β-unsaturated aldehydes like 4-hydroxynonenal (HNE) and acrolein, in that IsoLGs

[1]Division of Clinical Pharmacology, Vanderbilt University at Nashville, Nashville, Tennessee.
Departments of [2]Pathology and [3]Medicine, Vanderbilt University at Nashville, Nashville, Tennessee.
[4]Division of Cardiology, Department of Medicine, David Geffen School of Medicine at University of California Los Angeles, Los Angeles, California.
[5]GlycoMira Therapeutics, Salt Lake City, Utah.
[6]Department of Medicine, Oregon Health and Science University, Portland, Oregon.
[7]Department of Pharmacology, Vanderbilt University at Nashville, Nashville, Tennessee.
[8]Vanderbilt Institute of Chemical Biology, Vanderbilt University at Nashville, Nashville, Tennessee.

Innovation

These results identify isolevuglandin-modified phosphatidylethanolamine (IsoLG-PE) as a potent macrophage activator that acts as a novel ligand for receptor for advanced glycation endproducts and that is significantly elevated during conditions associated with inflammation. Thus, these studies suggest that interventions that lower IsoLG-PE levels or its activity may have a therapeutic benefit in atherosclerosis and other inflammatory diseases associated with lipid peroxidation.

predominantly react with primary amines such as the lysine moieties of protein or phosphatidylethanolamine (PE) rather than thiols such as the cysteine moieties of proteins or glutathione (8). Thus, the biological effects of IsoLGs are anticipated to markedly differ from those of HNE or acrolein.

Initial studies focused on the potential effects of protein modification by IsoLGs, as the rapid reaction of synthetic IsoLGs (most typically 15-E_2-IsoLG, as this represents one of the most abundantly formed regioisomers of IsoLGs) with purified proteins resulted in substantial protein adducts and loss of protein function (7, 8, 13, 21, 48, 58). Elevated levels of IsoLG protein adducts are found in a number of disease states, including cardiovascular disease (57), chronic kidney disease (57), Alzheimer's disease (14), hyperoxia (16), and allergic inflammation (65). In general, specific proteins that are modified during these conditions have not been identified, so the specific contributions of protein modification by IsoLGs to the pathogenesis of these diseases are largely unknown. Conceptually, modifications of proteins by IsoLGs that result in loss of function seem less likely to play a key role in disease than modifications of proteins or PE by IsoLGs that result in potent gain of function, since only a small percentage of the total number of copies of each protein or PE are modified.

Of particular relevance in this regard is our recent finding that PE modification by 15-E_2-IsoLG converts PE to a biologically active molecule that induces cytokine expression and adhesion molecule surface expression in endothelial cells (28). In this case, relatively low levels (1–3 μM) of PE modified by 15-E_2-IsoLG (IsoLG-PE) are needed for maximal response (28). Similarly, modification of PE by peroxidation of docosahexanoic acid (DHA) to form carboxyethyl pyrrole converts PE to a potent (low nM) activator of angiogenesis (66). Whether aldehyde-modified PEs exert direct effects on other cells that are important to inflammation, such as macrophages, is currently unknown.

Another reason that PE modification may be particularly relevant to the biological effects of IsoLGs is our finding that when exogenous 15-E_2-IsoLG is added to cultured cells, more PE is modified than protein lysyl residues (64). Similarly, more PE than protein is modified when IsoLGs are generated within lipoproteins *ex vivo* by their exposure to myeloperoxidase (27). This suggests that sufficient amounts of IsoLG-PE could be formed *in vivo* during inflammatory conditions associated with lipid peroxidation to be biologically relevant. However, to date, there is only one published study that has examined the levels of IsoLG-PE formed *in vivo* (42). This study showed that IsoLG-PE were elevated in the liver of mice during chronic ethanol consumption (a model of alcoholic liver disease) and in the plasma of human patients with macular degeneration. Thus additional studies are clearly needed to examine the levels of IsoLG-PE generated in other highly relevant inflammatory conditions associated with lipid peroxidation.

One such condition is familial hypercholesterolemia (FH), an autosomal dominant disorder characterized by severely elevated levels of low-density lipoprotein cholesterol (LDL-C) (55). FH patients have markedly increased inflammatory macrophage activation in the sub-intimal space of large arteries, resulting in increased risk of premature atherosclerotic cardiovascular disease (55). Because patients with FH have significantly higher levels of circulating myeloperoxidase (54) and oxidized lipids (15), it seems likely that they also have elevated levels of IsoLG-PE that might contribute to their inflammation.

Similarly, obesity induces significant systemic elevation in lipid peroxidation and is associated with a host of inflammatory conditions, including atherosclerosis, nonalcoholic steatohepatosis, and arthritis (6, 30, 38). Lipid accumulation in the liver and resulting inflammation appears to be a major driver of both hepatic and systemic insulin resistance (45). We and others have shown that high-fat diet feeding increases macrophage infiltration and expression of inflammatory genes in the liver (12). It therefore seems likely that high-fat feeding might elevate liver IsoLG-PE levels, which could then induce inflammatory responses in the liver and contribute to the development of steatohepatosis.

In addition to understanding the conditions that lead to IsoLG-PE formation *in vivo*, it would be highly valuable to understand the molecular mechanisms whereby IsoLG-PE and other aldehyde-modified PE exert their effects. For instance, does IsoLG-PE act simply by perturbing membrane structure or does it act on specific receptors? Identification of specific receptor(s) that mediated cellular responses to IsoLG-PE could greatly facilitate identification of relevant biological activities and signaling pathways.

To address these critical questions, we examined whether levels of IsoLG-PE increased under conditions associated with inflammatory disease, whether IsoLG-PE could activate the inflammatory response of macrophages, and whether specific receptors mediate this activity.

Results

IsoLG-PE levels are elevated in conditions associated with inflammation

For PE modification by IsoLGs to play an important role in the inflammation and macrophage activation associated with lipid peroxidation, the levels of IsoLG-PE would have to be elevated during these conditions. We therefore measured IsoLG-PE levels in two such conditions: hypercholesterolemia and hepatosteatosis associated with obesity. To examine whether IsoLG-PE levels were elevated by high cholesterol levels, we isolated plasma from FH patients before their undergoing LDL apheresis and in healthy volunteers. We found that IsoLG-PE levels were increased 76% in FH patients compared with control subjects (Fig. 1). To examine whether IsoLG-PE were elevated during the hepatosteatosis associated with obesity, we measured IsoLG-PE in the liver of mice fed a high-fat diet (60% of total calories) for 9 weeks (12). The mice fed the high-fat diet had

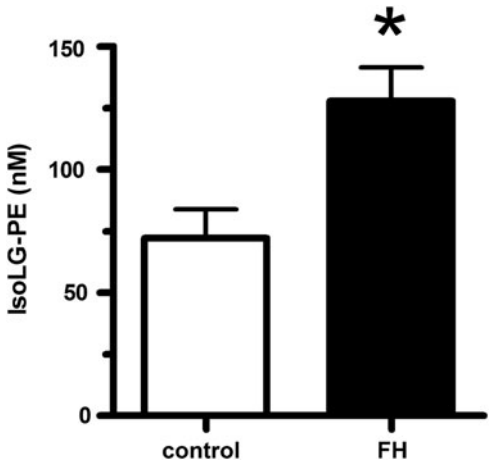

FIG. 1. IsoLG-PE is increased in the plasma of patients with FH. Plasma samples were obtained from healthy donors ($n=5$) and from FH patients ($n=5$). Collected plasma samples were treated with PLA_2 to generate lysoPE product, and the IsoLG-lysoPE-hydroxylactam species were quantified by LC/MS/MS as described in the Materials and Methods section. Mean ± SEM are shown, $*p=0.0143$ two-tailed Student's *t*-test. FH, familial hypercholesterolemia; IsoLG-PE, isolevuglandin-modified phosphatidylethanolamine; PLA_2, phospholipase A_2.

significantly higher liver weight (1.65 ± 0.30 g) than mice fed the low-fat chow diet (1.22 ± 0.03 g; $p<0.05$, two-tailed Student's *t*-test). Levels of IsoLG-PE per gram liver weight were 2.75-fold higher in mice fed the high-fat diet compared with those receiving the low-fat chow diet (Fig. 2). These results demonstrate that IsoLG-PE levels are increased during conditions associated with inflammation and macrophage activation.

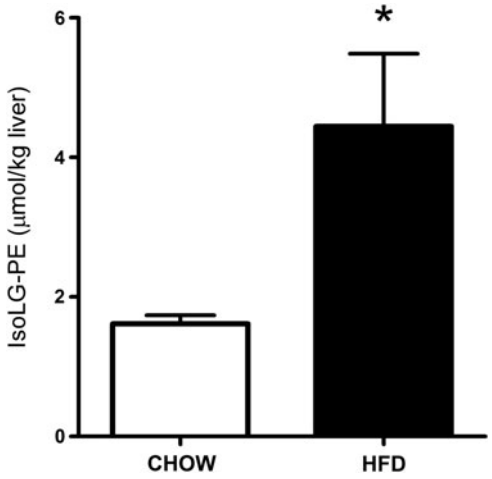

FIG. 2. IsoLG-PE is increased in the liver of mice fed a high-fat diet. Mice were fed a high-fat diet (60% fat from calories, $n=5$) or chow diet ($n=5$) for 9 weeks, and the livers were collected. Collected livers were treated with PLA_2 to generate lysoPE product, and IsoLG-lysoPE-hydroxylactam species were quantified by LC/MS/MS as described in the Materials and Methods section. Mean ± SEM for each group are shown, $*p=0.028$ two-tailed Student's *t*-test.

IsoLG-PE induces NFκB activation and inflammatory cytokine expression in macrophages

We have previously demonstrated that low micromolar concentrations of IsoLG-PE activated pro-inflammatory responses of endothelial cells, including increased expression of inflammatory cytokines and adhesion molecules (28). To examine whether IsoLG-PE also induced inflammatory gene expression in macrophages, we synthesized IsoLG-PE by reacting dipalmitoyl PE with 15-E_2-IsoLG and treated mouse macrophage RAW264.7 cells with this IsoLG-PE. When we measured mRNA expression of the inflammatory cytokines *Tnfa* and *Ccl2* (also known as *MCP-1*) by quantitative real-time PCR (qPCR), we found that 30 n*M* IsoLG-PE was sufficient to elicit maximal cytokine mRNA expression (Fig. 3A, B). To determine whether increased mRNA expression also increased protein expression, we then measured tumor necrosis factor-alpha (TNFα) protein levels in supernatant from RAW264.7 cells stimulated with IsoLG-PE, and again found that 30 n*M* IsoLG-PE was sufficient to elicit maximal TNFα protein expression (Fig. 3C). Addition of 15-E_2-IsoLG itself was not as potent at eliciting TNFα protein expression as adding IsoLG-PE (Fig. 3D), consistent with the notion that modification of PE rather than modification of other targets by IsoLG drives this inflammatory response.

Expression of *Tnfa* and *Ccl2* is typically downstream of nuclear factor kappa B (NFκB) activation, so we examined whether IsoLG-PE could elicit NFκB activation in RAW264.7 cells transfected with an NFκB luciferase reporter. We found that IsoLG-PE increased NFκB activity in a concentration-dependent manner with 30 n*M* IsoLG-PE being sufficient to elicit near maximal activation (Fig. 4A). A key step in the activation of NFκB is the phosphorylation of IκA and IκB by Iκ kinase β (IκKβ). Inhibition of IκKβ with 30 μ*M* PS-1145 inhibited TNFα expression induced by IsoLG-PE (Fig. 4B). These results are consistent with IsoLG-PE inducing inflammatory cytokine expression *via* NFκB signaling.

IsoLG-PE does not require hydrolysis to IsoLG-ethanolamine for activity

The ability of nanomolar concentrations of IsoLG-PE to activate macrophages suggested the possibility that IsoLG-PE acts as a ligand for receptor(s) on macrophages rather than by physical perturbation of membranes. Because we had previously found that IsoLG-PE is hydrolyzed to its ethanolamine analog (IsoLG-ETN) by the action of NAPE-PLD (29) and because NAPE-PLD is expressed in macrophages (75), we considered the possibility that hydrolysis of IsoLG-PE to IsoLG-ETN might be required to activate macrophages. If so, then IsoLG-ETN, rather than IsoLG-PE, would be the appropriate ligand to be used for receptor screening. We therefore compared the ability of IsoLG-PE and IsoLG-ETN to activate NFκB reporter expression. For these and subsequent experiments, we used passaged macrophages derived from bone marrow (BMDM) of mice where a luciferase reporter gene had been placed under the control of the NFκB-dependent promoter (nfkb-BMDM) (4). While both IsoLG-PE (Fig. 5A) and IsoLG-ETN (Fig. 5B) induced NFκB activation in a concentration-dependent manner, IsoLG-PE was more potent than IsoLG-ETN. We therefore used IsoLG-PE as a ligand for screening of the target

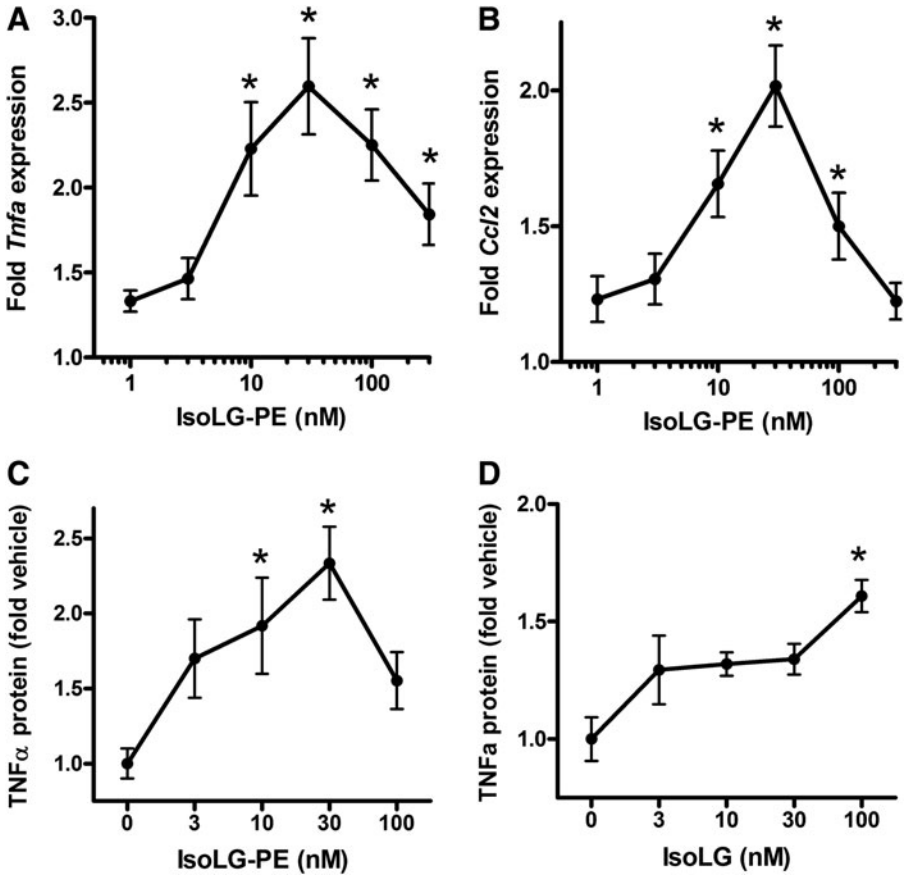

FIG. 3. IsoLG-PE induces gene expression of inflammatory cytokines in RAW264.7 mouse macrophages. Results are shown as mean ± SEM of all replicates from experiments on 3 separate days, $n = 4$ replicates per day, and normalized to expression in cells treated with 0.1 μM PE only. **(A)** *Tnfa* expression induced by IsoLG-PE as measured by qPCR. Results are shown as mean ± SEM of all replicates from experiments on 3 separate days, $n = 4$ replicates per day, and normalized to expression in cells treated with 0.1 μM PE only. One-way ANOVA, $p < 0.0001$, Dunnett's multiple-comparison test $^*p < 0.05$ *versus* 0.1 μM PE. **(B)** *Ccl2* (MCP-1) expression. Results are shown as mean ± SEM of all replicates from experiments on 3 separate days, $n = 4$ replicates per day, and normalized to expression in cells treated with 0.1 μM PE only. One-way ANOVA, $p < 0.0001$, Dunnett's multiple-comparison test $^*p < 0.05$ *versus* 0.1 μM PE. **(C)** TNFα protein expression induced by IsoLG-PE as measured by ELISA. Results are shown as mean ± SEM of all replicates from experiments on 2 separate days, $n = 3$ replicates per day, and normalized to expression in cells treated with vehicle only (0 nM IsoLG-PE). One-way ANOVA, $p < 0.008$, Dunnett's multiple-comparison test $^*p < 0.05$ *versus* 0 nM. **(D)** TNFα protein expression induced by 15-E_2-IsoLG as fold vehicle only (0 nM IsoLG) measured by ELISA. Results are shown as mean ± SEM of $n = 4$, normalized to expression in cells treated with vehicle only (0 nM IsoLG). One-way ANOVA, $p < 0.008$, Dunnett's multiple-comparison test $^*p < 0.05$ *versus* 0 nM. qPCR, quantitative real-time PCR; TNFα, tumor necrosis factor-alpha.

receptor. Of note, IsoLG-PE stimulated NFκB reporter about 10-fold less potently in nfkb-BMDM than in the RAW264.7 cell line. The reasons for this difference are unknown but may be the result of decreased expression of the cognate receptor or increased expression of NAPE-PLD or other lipases.

Identification of receptor for advanced glycation endproducts as an IsoLG-PE receptor

Proinflammatory lipids induce NFκB signaling in macrophages both by G-protein coupled receptors (GPCRs) such as the prostaglandin receptors and *via* pattern recognition receptors such as receptor for advanced glycation endproducts (RAGE), CD36, and Toll-like receptors (TLR). To determine whether IsoLG-PE was a ligand for GPCRs, we used 1 μM IsoLG-PE to screen a commercial panel (DiscoveRx, Fremont, CA) of cells expressing 154 individual GPCR with known ligands. One GPCR, the thromboxane A2 receptor (TxA2R), came up as a weak hit (25% activity of known ligand) in this screen (Supplementary Table S1; Supplementary Data are available online at www.liebertpub.com/ars). TxA2R is expressed on macrophages (1), and stimulation of this receptor with TxA2 stimulates NFκB expression (33). However, the TxA2R antagonist SQ29548 only modestly inhibited induction of NFκB activity (Supplementary Fig. S1) by IsoLG-PE, suggesting that TxA2R was not the primary receptor in macrophages mediating the response to IsoLG-PE.

Our failure to identify a GPCR for which IsoLG-PE served as a robust ligand led us to consider whether IsoLG-PE might primarily act instead *via* pattern recognition receptors. In particular, we chose to focus on the RAGE, as this pattern recognition receptor initiates NFκB signaling in response to ligands such as aldehyde-modified peptides and

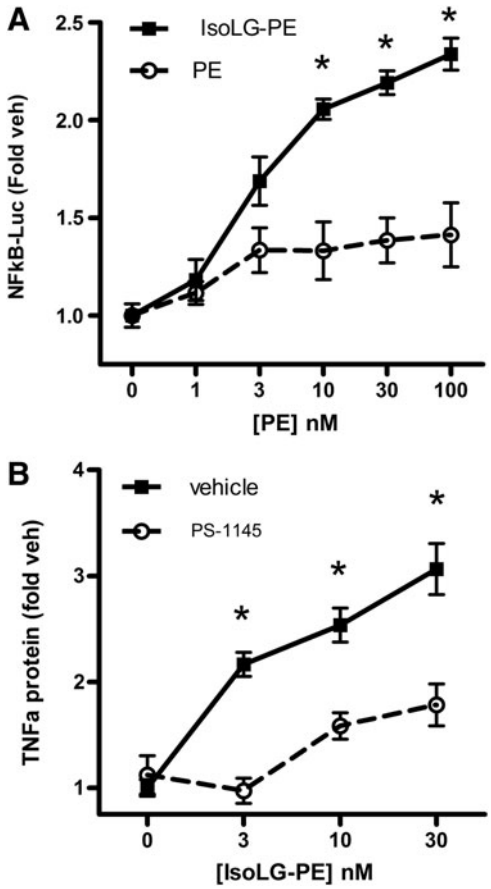

FIG. 4. IsoLG-PE activates NFκB to induce TNFα in RAW264.7 cells. (A) Effects of IsoLG-PE and PE on NFκB reporter activity in transfected RAW264.7 murine macrophages. Results are shown as mean ± SEM, $n = 4$ replicates and normalized to expression in vehicle-treated cells (0 n*M*), Two-way ANOVA, $p < 0.0001$ for concentration, treatment, and interaction, $^*p < 0.05$ for IsoLG-PE *versus* PE, Bonferroni's multiple-comparisons test for the same concentration of each phospholipid. **(B)** PS-1145 inhibition of NFκB activator IκKβ blocks IsoLG-PE induction of TNFα protein expression. Results are shown as mean ± SEM of all replicates from experiments on 2 separate days, $n = 3$–4 replicates per day, and normalized to expression in cells treated with vehicle (0 n*M*) on that day. Two-way ANOVA, $p < 0.0001$, concentration and treatment. $^*p < 0.01$ Bonferroni's multiple-comparisons test for vehicle *versus* PS-1145 for the same concentration of IsoLG-PE. IκKβ, Iκ kinase β; NFκB, nuclear factor kappa B.

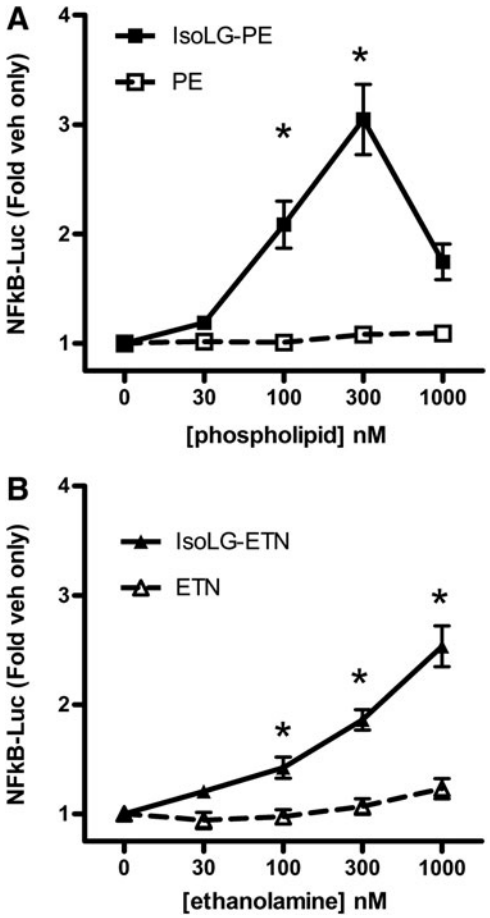

FIG. 5. IsoLG-PE and its metabolite IsoLG-ETN activate NFκB-luciferase reporter expression in bone marrow-derived macrophages from transgenic NFκB reporter mice (nfkb-BMDM). Results are shown as mean ± SEM of all replicates from experiments on a minimum of 3 separate days, $n = 4$–6 independent replicates per day, and normalized to expression in vehicle-treated cells. **(A)** Effects of IsoLG-PE and PE on NFκB reporter expression activity. Two-way ANOVA, $p < 0.0001$, treatment, $p = 0.0008$ concentration; $^*p < 0.01$, Bonferroni's multiple-comparisons test IsoLG-PE *versus* PE for the same concentration. **(B)** Effects of IsoLG-ETN and ETN on NFκB reporter expression activity. Two-way ANOVA, $p < 0.0001$, treatment, concentration; $^*p < 0.01$, Bonferroni's multiple-comparisons test IsoLG-ETN *versus* ETN for the same concentration. IsoLG-ETN, isolevuglandin-modified ethanolamine.

anionic phospholipids that share some structural features with IsoLG-PE (Fig. 6). The soluble form of RAGE (sRAGE) acts as a decoy peptide to inhibit RAGE signaling, because sRAGE binds the same ligands as full-length RAGE but lacks its intracellular signaling domains (19, 23). We found that preincubation of IsoLG-PE with 2 mg/L of sRAGE markedly inhibited the ability of IsoLG-PE to induce NFκB activation (Fig. 7A). To test whether RAGE was required for IsoLG-PE-induced signaling, we examined the effect of two RAGE antagonists with differing modes of action on IsoLG-PE activation of macrophages. We found that GM-0111, a synthetic glycosaminoglycan previously shown to act as an RAGE antagonist (73), significantly inhibited IsoLG-PE-induced NFκB reporter activity (Fig. 7B). We also found that FPS-ZM1, a high-affinity antagonist that specifically binds the V domain of RAGE (18), markedly inhibited IsoLG-PE-induced NFκB reporter activity (Fig. 7C).

These experiments suggested that IsoLG-PE activated NFκB and inflammatory cytokine secretion *via* RAGE. To further examine the requirement for RAGE in IsoLG-PE activation of macrophages, we isolated macrophages from the bone marrow of wild-type (C57BL6J) mice and *Ager* null mice that lack RAGE and examined whether IsoLG-PE could activate cytokine expression in these macrophages. BMDM

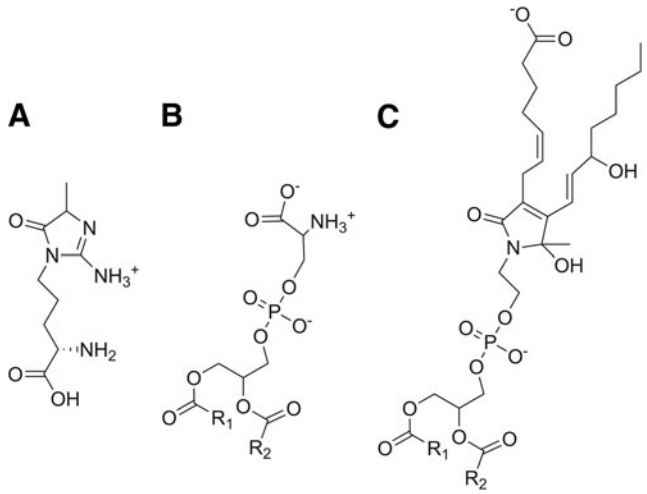

FIG. 6. Chemical structures of known RAGE ligands and IsoLG-PE. (A) The advanced glycation endproduct hydroimidazolone adducts derived from methylglyoxal reaction with arginine (MG-Hs), **(B)** phosphatidylserine, and **(C)** IsoLG-PE. RAGE, receptor for advanced glycation endproducts.

were chosen for these experiments, as they could be readily obtained from both wild-type and Ager null mice and BMDM have been widely used for studying the effects of pattern recognition receptors both *in vitro* and *in vivo*. In contrast to BMDM from wild-type mice, BMDM from *Ager* null mice failed to induce inflammatory cytokines in response to IsoLG-PE (Fig. 8).

Discussion

Our findings that IsoLG-PE levels are elevated in conditions associated with lipid peroxidation and inflammation, that IsoLG-PE activates NFκB and inflammatory cytokine expression at nanomolar concentrations, and that IsoLG-PE requires RAGE to induce macrophage activation implicate IsoLG-PE and RAGE as mediators of inflammation induced by lipid peroxidation.

A significant body of literature has previously demonstrated that risk factors for inflammatory diseases such as hypercholesterolemia and obesity increase lipid peroxidation (5, 15, 63). However, the extent to which IsoLG-PE levels are elevated during inflammatory conditions has been largely unknown, as only one previous study had measured IsoLG-PE levels *in vivo*. Li *et al.* found that feeding mice ethanol chronically, a condition that elevates lipid aldehydes including malondialdehyde and 4-hydroxynonenal (22), markedly increases hepatic levels of IsoLG-PE (42). They also showed increased plasma levels with macular degeneration, a condition previously established to increase levels of lipid aldehydes, including malondialdehyde and 4-hydroxynonenal (40).

Our findings suggest that a wide variety of conditions associated with lipid peroxidation are likely to elevate IsoLG-PE levels. For instance, we found that IsoLG-PE was markedly increased in plasma of FH patients. While future studies will be needed to elucidate the exact mechanisms underlying this increase in IsoLG-PE levels, we note that this inherited disorder is associated with markedly increased myeloperoxidase activity (54). Increased myeloperoxidase activity may be relevant, because Poliakov *et al.* previously showed that exposure to myeloperoxidase generated significant amounts of IsoLG protein adduct both *in vitro* and *in vivo* (53), and we

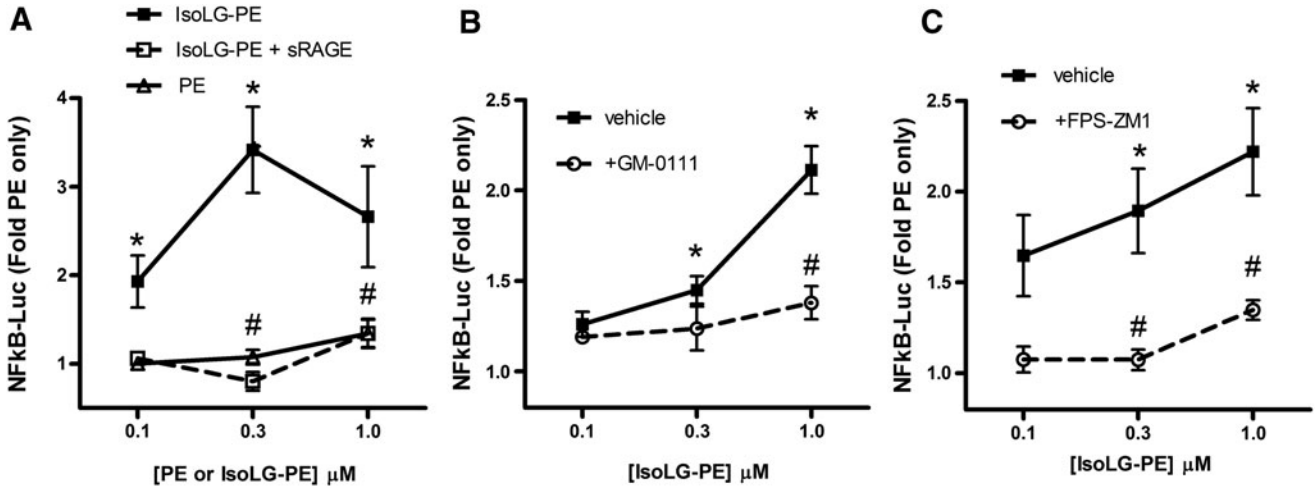

FIG. 7. Effects of IsoLG-PE are dependent on RAGE. (A) sRAGE (2 mg/L) inhibits activation of NFκB by IsoLG-PE. Results are shown as mean ± SEM of all replicates from experiments on 2 separate days, $n = 4$ independent replicates per day, and normalized to expression in cells treated with 0.1 μM PE only. One-way ANOVA, $p < 0.0001$, Bonferroni's multiple-comparisons test $^{*}p < 0.05$ *versus* 0.1 μM PE, $^{\#}p < 0.05$ for sRAGE treatment *versus* nontreatment with the same concentration of IsoLG-PE. **(B)** The synthetic glycosaminoglycan, GM-0111 (100 μM), that acts as an antagonist of RAGE also inhibits NFκB activation by IsoLG-PE. One-way ANOVA, $p < 0.0001$, Bonferroni's multiple-comparisons test $^{*}p < 0.05$ *versus* 0.1 μM PE, $^{\#}p < 0.05$ for GM-0111 treatment *versus* nontreatment with the same concentration of IsoLG-PE. **(C)** The high-affinity RAGE-specific antagonist, FPS-ZM1 (0.2 μM) inhibits IsoLG-PE-induced NFκB reporter activity. Results are shown as mean ± SEM of all replicates from experiments on 3 separate days, $n = 4$–5 independent replicates per day. One-way ANOVA, $p < 0.0001$, Bonferroni's multiple-comparisons test $^{*}p < 0.05$ *versus* 0.1 μM PE, $^{\#}p < 0.05$ for FPS-ZM1 treatment *versus* nontreatment with the same concentration of IsoLG-PE. sRAGE, soluble form of receptor for advanced glycation endproducts.

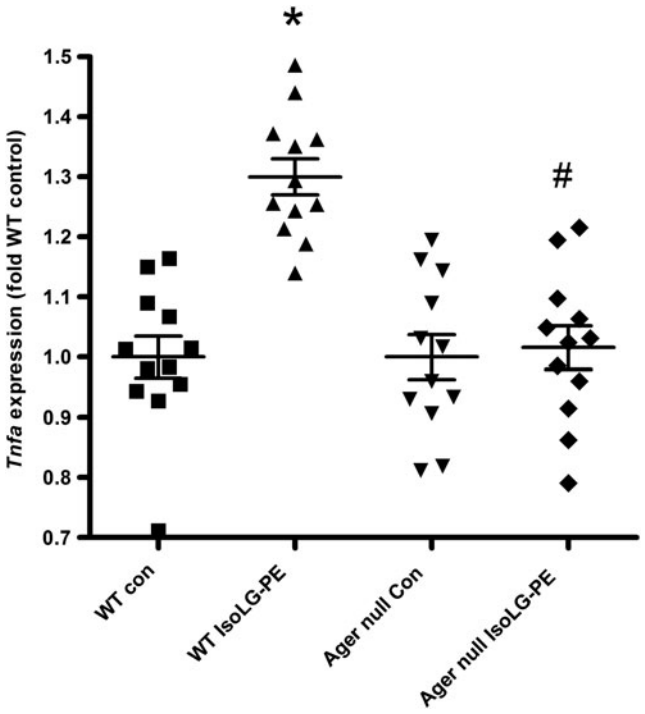

FIG. 8. Bone marrow-derived macrophages derived from wild-type mice (WT), but not *Ager* null mice, induce *Tnfa* mRNA expression in response to 0.3 μ*M* IsoLG-PE. Results are shown as mean ± SEM of all replicates on 2 separate days, $n = 6$ replicates per day, with each replicate representing cells derived from independent femur, and normalized to expression in wild-type control-treated cells. One-way ANOVA $p < 0.0001$, Bonferroni's multiple-comparison test $^{*}p < 0.05$ *versus* WT control-treated cells, $^{\#}p < 0.05$ for WT cells treated with IsoLG-PE *versus* Ager null treated with IsoLG-PE.

showed that exposure of lipoprotein to myeloperoxidase *in vitro* generated IsoLG-PE (27). FH is associated with markedly increased inflammation (50) and risk for atherosclerosis (10). Our findings suggest that generation of IsoLG-PE and subsequent activation of macrophages by IsoLG-PE may be one mechanism underlying this inflammation, but future studies will be needed to test whether reducing IsoLG-PE levels also reduces inflammation in FH patients.

Our finding that IsoLG-PE levels were also elevated in the liver of mice fed a high-fat diet supports the notion that generation of IsoLG-PE may be a consistent feature of inflammation associated with lipid peroxidation. Obesity is a well-established risk factor for inflammatory diseases associated with increased lipid peroxidation such as steatohepatitis, atherosclerosis, and arthritis (2, 46, 67). The infiltration and activation of macrophages into the liver during development of obesity is considered a critical feature of metabolic syndrome and may play an important role in the development of insulin resistance and vascular disease associated with metabolic syndrome (6). Additional studies are needed to determine whether reducing IsoLG-PE levels in the liver will mitigate the effects of high-fat feeding on liver macrophage activation, insulin resistance, and liver injury. In this regard, it is important to note that while increasing NAPE-PLD activity could reduce IsoLG-PE levels, IsoLG-ETN was about threefold less potent than IsoLG-PE. Thus, accumulation of IsoLG-ETN could also contribute to inflammation, and it would be important to confirm that any potential therapeutic intervention markedly reduced both IsoLG-PE and IsoLG-ETN levels.

The potential biological significance of elevated IsoLG-PE levels is shown by our finding that IsoLG-PE potently activates NFκB and expression of *Tnfa* and *Ccl2* in macrophages. Activation of macrophages is a key step in many inflammatory diseases such as atherosclerosis and steatohepatitis and elevated *Tnfa* and *Ccl2* (*MCP-1*) levels in these diseases is well established (25, 32, 43). TNFα is a master regulator of inflammation and induces expression of cytokines, prostaglandins, platelet-activating factor, adhesion molecules, inducible nitric oxide synthase, and matrix metalloproteinases (52, 56, 74). The importance of macrophage secretion of TNFα in atherogenesis was shown by studies where transplantation of *Apoe* null/*Tnfa* null bone marrow into *Apoe* null receipt mice gave rise to lesions that were 83% smaller than transplantation of *Apoe* null-only bone marrow into Apoe null receipt mice (9). CCL2 is similarly important in atherogenesis, because mice lacking either *Ccl2* or its receptor, *Ccr2*, develop lesions that are significantly reduced in size (17, 26). Thus, the ability of IsoLG-PE to activate *Tnfa* and *Ccl2* expression by cultured macrophages suggests that IsoLG-PE may be an important inducer of macrophage TNFα and CCL2 secretion in FH and fatty liver disease.

Another key question our studies sought to answer was whether the effects of IsoLG-PE are mediated by specific receptors rather than simply due to membrane perturbations. At micromolar concentrations, IsoLG-PE markedly lowers the liquid crystalline to hexagonal phase transition temperature of liposomes and also induces endoplasmic reticulum (ER) stress responses in cultured endothelial cells (28), consistent with membrane perturbation exerting biological effects. However, the endothelial response can only be partially reversed by inhibition of ER stress, suggesting a role for other mechanisms besides membrane perturbation. Our finding that concentrations of IsoLG-PE (30 n*M*), which are well below that required to markedly perturb overall membrane structure, were sufficient to induce maximal inflammatory responses in murine macrophages strongly implicates receptor-driven mechanisms.

Our finding that soluble RAGE, RAGE antagonists, and genetic deletion of RAGE block the effects of IsoLG-PE in macrophages strongly implicate RAGE as an IsoG-PE receptor. Multiple ligands are known to activate RAGE, including advanced glycation endproducts (AGEs), S100 family proteins, high mobility group protein box-1 (HMGB1), amyloid β, and phosphatidylserine (19, 34). Common features of previously characterized RAGE ligands are a negative charge at neutral pH and an ability to drive RAGE oligimerization by forming multimers (19). Most RAGE ligands bind at a patch of positively charged residues formed by the V and C1 domains of RAGE and this binding stabilizes preassembled complexes of multiple RAGE monomers (39), allowing diaphanous-1 to bind and activate downstream signals, including ERK, JNK, p38, and NFκB (37). IsoLG-PE is also negatively charged and may form oligomers in the sense that closely adjacent PE are likely to undergo IsoLG modification. IsoLG-PE shares partial structural features with methylglyoxal-hydroimidazolones (MG-Hs) (Fig. 6), which

bind RAGE with high-affinity (Kd 40 n*M*) (70) and are the most potent of the AGE class of RAGE ligands. IsoLG-PE also shares the same phosphatidyl moiety as the recently described RAGE ligand phosphatidylserine (34). Additional studies will be needed to identify the specific binding sites of IsoLG-PE on RAGE and the mechanisms underlying its activation of RAGE signaling complexes.

Our finding that IsoLG-PE activates RAGE on macrophages suggests that activation of RAGE may be responsible for the effects of IsoLG-PE or IsoLG seen in other cell types. For instance, IsoLG-PE activates the surface expression of adhesion molecules and expression of inflammatory cytokines in endothelial cells (28) and IsoLG added to platelets causes their activation and aggregation (3). RAGE is found on both of these cell types (20, 60), so that these activities might plausibly be mediated by RAGE. In particular, activation of RAGE on endothelial cells could explain our previous finding that IsoLG-PE induces the ER stress response of endothelial cells (28), similar to RAGE agonists such as HMGB1 that induce ER stress (44).

One feature of our findings that needs further investigation is why there are significant differences in the potency of IsoLG-PE between various cell types. For instance, IsoLG-PE induced NFκB activation about 10 times more potently in RAW264.7 macrophages (30 n*M*) than in bone marrow-derived macrophages (300 n*M*). For endothelial cells, 3 μM IsoLG-PE was required for maximal induction of inflammatory effects. These differences in sensitivity to IsoLG-PE might reflect differences between cell types in NAPE-PLD expression, RAGE surface expression, or interactions of RAGE with other receptors. Several RAGE ligands interact with other pattern recognition receptors such as CD36 and TLR4 (35, 36, 51, 69), and activation of these other receptors can increase RAGE expression. Because we found that the thromboxane receptor antagonists SQ29548 modestly inhibited IsoLG-PE activation of NFκB, we also cannot rule out that RAGE and the thromboxane receptor act synergistically in some manner to invoke responses in the macrophages.

Our identification of RAGE as the first known receptor for IsoLG-PE provides insight into ways in which IsoLG-PE might act *in vivo*. RAGE is an important mediator of inflammatory responses and has been implicated in atherosclerosis and inflammation associated with hypercholesterolemia and a high-fat diet. For instance, genetic deletion of *Ager* decreases atherosclerosis in both nondiabetic and diabetic *Apoe* null mice (31, 62). *Ager* null mice also show decreased obesity, adipose tissue inflammation, and insulin resistance in wild-type C57BL6 mice fed a high-fat diet (61). RAGE expressed on bone marrow-derived cells (*e.g.*, monocyte/macrophages) specifically contributes to atherosclerosis, as transplantation of *Ager* null/*Apoe* null bone marrow into *Apoe* null mice results in markedly reduced atherosclerosis compared with those receiving bone marrow from *Ager*-positive *Apoe* null mice (47). Administration of sRAGE markedly decreases atherosclerosis and oxidative injury in animal models (11, 41, 68, 71, 72). Thus, activation of RAGE by IsoLG-PE could plausibly contribute to the development of atherosclerosis and liver disease associated with hypercholesterolemia or obesity. Future studies examining the effect of therapeutic interventions that lower IsoLG-PE levels in these diseases will be needed to investigate this potential contribution.

Materials and Methods

Materials

The following reagents were purchased commercially: 1,2-dipalmitoyl-*sn*-glycero-3-phosphoethanolamine (DPPE; Avanti Polar Lipids, Alabaster, AL), ethanolamine (ETN; Sigma-Aldrich, St. Louis, MO), phospholipase A_2 (PLA_2) isolated from honey bee venom (Sigma-Aldrich), antibiotic-antimycotic mix (Gibco by Life Technologies, Rockville, MD), IQ SYBR Green supermix and iScript cDNA Synthesis Kit (Bio-Rad, Hercules, CA), SQ29548 (Cayman Chemicals, Ann Arbor, MI), and organic solvents, including methanol, chloroform, dichloromethane, and acetonitrile, were high-performance liquid chromatography grade (Sigma-Aldrich).

IsoLG-PE and IsoLG-ETN were synthesized by a reaction with DPPE and ETN with 15-E_2-IsoLG as previously reported (28, 64). It is important to note that 15-E_2-IsoLG is only one out of the eight regioisomers (5-E_2-IsoLG, 5-D_2-IsoLG, 8-E_2-IsoLG, 8-D_2-IsoLG, 12-E_2-IsoLG, 12-D_2-IsoLG, 15-E_2-IsoLG, and 15-D_2-IsoLG) that are potentially generated by peroxidation of arachidonic acid. Based on theoretical considerations, the 15- and 5-series IsoLGs are expected to be formed in significantly greater abundance than the 8- or 12-series IsoLGs. Levuglandin E_2 (LGE_2) formed nonenzymatically from prostaglandin H_2 is chemically identical to 15-E_2-IsoLG. For these reasons, 15-E_2-IsoLG has been the most widely used regioisomer of IsoLG synthesized for use in studies. The synthesis of C17:0NAPE was adapted from (24) with a modified purification method (28).

Plasma from FH patients

Ethylenediaminetetraacetic acid (EDTA) plasma was isolated from blood of FH patients ($n=5$) before undergoing LDL apheresis. Two patients were FH homozygotes and three patients had severe heterozygous FH with LDL-C >200 mg/dl before each LDL apheresis session. As a control, EDTA plasma was isolated from blood of healthy volunteers ($n=5$). The study protocol was approved by the Vanderbilt University Medical Center institutional review board (IRB 101615). All participants gave informed consent.

Animal studies

All animal experiments were performed according to protocols approved by the Institutional Animal Care and Use Committee at Vanderbilt University. In a previously published study (12), we showed that prolonged feeding of a high-fat diet induced major hallmarks of hepatosteatosis, including triglyceride accumulation, macrophage infiltration, and expression of inflammatory genes [Figs. 4 and 5 of Ref. (12)]. In that same study, we fed 6-week-old male C57BL/6J mice a standard low-fat chow diet (Lab Diet 5001 13.5% kcal from fat, 60% kcal from carbohydrate, 28.5% kcal from protein; TestDiet, St. Louis, MO) or a high-fat diet (Test-Diet® 58Y1, containing 60% fat by kcal; TestDiet) for 9 weeks and reported that the high-fat fed mice had significantly higher fasting glucose and insulin levels and impaired glucose tolerance than mice fed a low-fat chow diet [Fig. 11 of Ref. (12)]. After the 9 weeks of feeding, the mice were euthanized, the livers were harvested, and aliquots were stored at $-80°C$ until analysis for this study. The mice fed the high-fat diet had higher body weight (37.52 ± 0.74 g) and

total body fat (12.14 ± 0.45 g) than mice fed the low-fat chow diet (25.80 ± 0.27 g body weight and 2.61 ± 0.10 g body fat, respectively; $p < 0.05$ for each parameter, two-tailed Student's *t*-test). Body weight was measured using a portable electronic scale. For body composition, mice were scanned by magnetic resonance imaging using a Bruker Minispec MQ10 NMR Analyzer to determine fat mass, lean mass, and free fluid.

Femurs from *Ager* null mice (two each from three individual mice, 6 months old) were a kind gift from Dr. Tim Oury, Department of Pathology, University of Pittsburgh and femurs collected from C57BL/6J male mice of a similar age were used as a control. For isolation of bone marrow-derived macrophages, femurs were harvested from euthanized mice and shipped in RPMI 1640 with 2% fetal bovine serum (FBS), 10 units/ml heparin, pencillin, and streptomycin at 4°C. After cutting off muscles, the ends of the femur were cut off and the bone marrow cells were carefully flushed out. Cells were resuspended by gentle pipetting and passed through a 70 μm filter into a 50 ml conical tube. Cells were collected by centrifugation and resuspended in 8 ml Dulbecco's modified Eagle's medium (DMEM) (per femur) with 10% FBS, 1 × antibiotic-antimycotic, and 20 ng/ml macrophage colony-stimulating factor. One milliliter of cells was transferred to 1 well of a 12-well plate and incubated at 37°C in 5% CO_2 atmosphere. Medium was changed every 2 days after first culture, and cells were used for experiments on day 7 and 10 when cells were 85%–90% confluent.

Measurement of IsoLG-PE in tissues

IsoLG-PE levels were measured by LC-MS/MS with a modified PLA_2 assay (42). Plasma samples were vortexed with chloroform/methanol (2/1, v/v) containing 0.1% BHT. Liver tissues were homogenized manually in a tube with chloroform/methanol (2/1, v/v) containing 0.01% BHT. C17NAPE (0.1 nmol) was added as an internal standard. After incubation at 4°C for 1 h, a 1/3 volume of phosphate-buffered saline (PBS) was added, the mixture was centrifuged at 3000 rpm for 15 min, and the lower organic layer containing the lipids was collected and evaporated under a stream of nitrogen. After being re-dissolved in 1 ml of chloroform, lipids were loaded onto a Sep-Pak silica cartridge (Waters Corp., Milford, MA) pre-equilibrated with chloroform, the cartridge was washed with 8 ml of chloroform, and IsoLG-PE was eluted by 8 ml of 50% methanol/chloroform. The lipids were dried under nitrogen and stored at −80°C before hydrolysis and analysis. The lipid extract was re-dissolved in methanol (50 μl) followed by the addition of a PBS solution (10 m*M*, pH 7.4, 450 μl) containing $CaCl_2$ (5 m*M*). Phospholipase A_2 from honey bee venom (PLA_2, 10 units/sample) was added, incubated under argon at 37°C overnight, and extracted with 1.5 ml of chloroform/methanol (2/1, v/v). Solvents were evaporated and the lipid was re-dissolved in methanol (50 μl) and analyzed by LC/MS/MS using a ThermoFinniganQuantum electrospray ionization triple-quadrupole mass spectrometer (Thermo Fisher Scientific, Waltham, MA) operating in negative-ion multiple reaction monitoring mode.

Mobile phase A consisted of 1 m*M* ammonium acetate in water/acetonitrile/methanol (1/1/3), and mobile phase B consisted of 1 m*M* ammonium acetate in ethanol. The lipids were chromatographed on a Zorbax XDB-C8 column (50 × 2.1 mm; Agilent Tech., Santa Clara, CA) with a constant flow rate of 400 μl/min. After a 0.5 min hold at 1% mobile phase B, the solvent was gradient ramped to 99% B over 6 min, held at 99% B for 1 min, returned to 1% B over 1 min, and held for 1 min before the next injection. The electrospray needle was used at −3300 V. The ion-transfer tube was operated at −35 V and 270°C. The tube lens voltage was set to −180 V. Mass transitions of *m/z* 704.3 → 255.1 for C17:0NAPE, *m/z* 798.3 → 153.0 for IsoLG-(C16:1)lysoPE, *m/z* 800.3 → 153.0 for IsoLG-(C16:0)lysoPE, *m/z* 824.3 → 153.0 for IsoLG-(C18:2)lysoPE, *m/z* 826.3 → 153.0 for IsoLG-(C18:1)lysoPE, and *m/z* 828.3 → 153.0 for IsoLG-(C18:0)lysoPE were monitored, with a collision energy of 50 eV. The chromatographic results were processed in Xcaliber software (Thermo Fischer Scientific, Waltham, MA) using nine-point Gaussian smoothing, and the peak heights in comparison to the internal standard were used to calculate the amount of each species present in the sample. Linear regression and correlation analysis was performed using GraphPad Prism (version 4.00 for Windows; GraphPad Software, San Diego, CA). For plasma, significant signal for IsoLG-(C16:0)lysoPE only was detected, so only this species was used for quantitation. For liver, significant signals for IsoLG-(C16:1)lysoPE, IsoLG-(C16:0)lysoPE, IsoLG-(C18:2)lysoPE, and IsoLG-(C18:1)lysoPE were detected, so the sum of these species in each sample was used for quantitation. Representative chromatographs from liver of chow and high-fat fed mice are shown in Supplementary Figure S2.

Cell culture

RAW264.7 macrophage cells (American Type Cell Culture, Manassas, VA) were cultured in 100 mm dishes with DMEM supplemented with 10% FBS and 1 × antibiotic-antimycotic mix until 85%–90% confluent. Cells from confluent plates were trypsinized, transferred to six 24-well plates (1 ml each well), and cultured for 48 h before use. RAW264.7 cells transfected with NFκB reporter were a kind gift from Dr. Claus Schneider, Vanderbilt University. These cells were generated by transfection with plasmid from Takara Clontech containing an NFκB enhancer element 5′ to a minimal promoter driving expression of secreted *Metridia* luciferase reporter, as well as kanamycin/neomycin resistance gene. Transfected cells were selected with 1 mg/ml geneticin in DMEM supplemented with 10% FBS and 1 × antibiotic-antmycotic mix.

Established NFκB reporter macrophages originally derived from bone marrow of transgenic mice expressing a reporter plasmid containing a total of eight NFκB-binding sites upstream of the herpes simplex virus minimal thymidine kinase promoter driving expression of *Photinus* luciferase (18) were a kind gift from Dr. Timothy S. Blackwell, Vanderbilt University. These passaged nfkb-BMDM were used for the majority of NFκB reporter experiments instead of transfected RAW264.7 cell line, because nfkb-BMDM were readily available and relatively easy to use to produce the large numbers of reporter cells needed for our assays, and because these nfkb-BMDM have been widely used in studies examining NFκB signaling, including studies examining the effects of reactive lipids on NFκB signaling (49). All cells were grown to 85%–90% confluence in 100 mm dishes containing DMEM containing 10% fetal bovine serum,

1× antibiotic-antimycotic mix, trypsinized, and cells from each plate were aliquoted to six 12-well culture dishes, cultured for 48 h, and incubated in the same medium with serum overnight before experiments.

Cytokine mRNA expression

RAW264.7 macrophage cells were stimulated with either PE (100 n*M*) or IsoLG-PE (1–300 n*M*) in Hanks' buffered saline solution (HBSS) with 0.1% human serum albumin and 0.2% dimethyl sulfoxide (DMSO) at 37°C for 4 h. The media was then removed, and macrophages were washed with cold PBS. RLT buffer was added, and the plates were incubated on ice for 30 min. The lysate was collected and RNA was extracted with RNeasy Mini kit (Qiagen, Valencia, CA) for PCR analysis. Levels of *Actb* (internal standard), *Tnfa*, and *Ccl2* mRNAs were measured after conversion to cDNA (with iScript cDNA Synthesis Kit) by qPCR using IQ SYBR Green supermix. The primer pairs were purchased from Sigma-Aldrich as follows: (a) *Actb*: sense GAG CGC AAG TAC TCT GTG TG, antisense CGG ACT CAT CGT ACT CCT G; (b) *Tnfa* (Sigma-Aldrich): sense CCA TTC CTG AGT TCT GCA AAG, antisense GCA AAT ATA AAT AGA GGG C; and (c) *Ccl2*: sense ACT GAA GCC AGC TCT CTC TTC CTC, antisense TTC CTT CTT GGG GTC AGC ACA GAC. Results are shown as the average of 3 separate experimental days, four replicate wells per day, normalized to PE-treated cells. Bone marrow-derived macrophages from wild-type and *Ager* null mice were stimulated with either vehicle or 300 n*M* IsoLG-PE for 4 h, and *Tnfa* expression was measured by qPCR as described earlier.

TNFα protein expression

Supernatant from RAW264.7 cells treated with IsoLG-PE, IsoLG, or vehicle (HBSS with 0.1% human serum albumin and 0.2% DMSO for IsoLG-PE and 0.02% DMSO for IsoLG) overnight were collected and measured using a commercial mouse TNFα DuoSet ELISA assay kit (R&D Systems, Minneapolis, MN).

NFκB reporter activity

RAW264.7 NFκB reporter or nfkb-BMDM cells were washed twice with HBSS to remove serum and then treated with IsoLG-PE, IsoLG-ETN, PE, or vehicle (HBSS with 0.1% human serum albumin and 0.2% DMSO) for 30 min at 37°C. Cell media was then removed, Luciferase Assay Reporter Lysis Buffer (Promega, Madison, WI) was added, and the resulting bioluminescence was quantified and normalized to control.

For studies examining the effects of sRAGE, IsoLG-PE was preincubated with vehicle (HBSS with 0.1% HSA) or sRAGE (2 mg/L) for 37°C for 1 h before treatment of cells. For these experiments, 0.1 μM PE in vehicle was used as a control, and bioluminescence was normalized to 0.1 μM PE. For studies examining the effects of RAGE antagonists, cells were treated with either vehicle (HBSS), 0.2 μM FPS-ZM1 (Calbiochem, San Diego, CA), or 100 μM GM-0111 (Glyco-Mira, Salt Lake City, UT) along with IsoLG-PE or PE in HBSS with 0.1% human serum albumin and 0.2% DMSO at 37°C for 30 min and resulting bioluminescence was normalized to cells treated with 0.1 μM PE.

Screen of GPCR library

IsoLG-PE was synthesized as described earlier and purified from unreacted PE by HPLC with the fractions where IsoLG-PE eluded identified by LC/MS/MS and combined. The solvent was evaporated under nitrogen, and the IsoLG-PE was redissolved in DMSO at 100 μM for shipment to DiscoveRx for screening at 1 μM final concentration of IsoLG-PE using their proprietary functional Cell-Based GPCR Assay Panel with β-arrestin recruitment as the readout. In agonist mode for GPCR receptors with known ligands, the extent of GPCR activation by test compound is calculated based on maximal activation with known ligand.

Acknowledgments

This work was supported in part by grants from National Institutes of Health HL111945, HL116263, HL30568, HL34343, AT0007830, ES000267, and RR024975 and by the Laubisch, Castera, and M.K. Grey Funds at the UCLA. The authors have no other financial interests to disclose. They thank Dr. Tim Oury for the kind gift of femurs harvested from *Ager* null mice and Dr. Timothy Blackwell for established bone marrow-derived macrophages from NFκB reporter mice. They also thank Dr. Olivier Boutaud for helpful discussions about thromboxane receptor antagonists and activation.

Author Disclosure Statement

No competing financial interests exist.

References

1. Allan CJ and Halushka PV. Characterization of human peripheral blood monocyte thromboxane A2 receptors. *J Pharmacol Exp Ther* 270: 446–452, 1994.
2. Bartels ED, Bang CA, and Nielsen LB. Early atherosclerosis and vascular inflammation in mice with diet-induced type 2 diabetes. *Eur J Clin Invest* 39: 190–199, 2009.
3. Bernoud-Hubac N, Alam DA, Lefils J, Davies SS, Amarnath V, Guichardant M, Roberts Ii LJ, and Lagarde M. Low concentrations of reactive [gamma]-ketoaldehydes prime thromboxane-dependent human platelet aggregation *via* p38-MAPK activation. *Biochim Biophys Acta* 1791: 307–313, 2009.
4. Blackwell TS, Yull FE, Chen CL, Venkatakrishnan A, Blackwell TR, Hicks DJ, Lancaster LH, Christman JW, and Kerr LD. Multiorgan nuclear factor kappa B activation in a transgenic mouse model of systemic inflammation. *Am J Respir Crit Care Med* 162: 1095–1101, 2000.
5. Bochkov VN, Oskolkova OV, Birukov KG, Levonen AL, Binder CJ, and Stockl J. Generation and biological activities of oxidized phospholipids. *Antioxid Redox Signal* 12: 1009–1059, 2010.
6. Boppidi H and Daram SR. Nonalcoholic fatty liver disease: hepatic manifestation of obesity and the metabolic syndrome. *Postgrad Med* 120: E01–E07, 2008.
7. Brame CJ, Boutaud O, Davies SS, Yang T, Oates JA, Roden D, and Roberts LJ, 2nd. Modification of proteins by isoketal-containing oxidized phospholipids. *J Biol Chem* 279: 13447–13451, 2004.
8. Brame CJ, Salomon RG, Morrow JD, and Roberts LJ, 2nd. Identification of extremely reactive gamma-ketoaldehydes

(isolevuglandins) as products of the isoprostane pathway and characterization of their lysyl protein adducts. *J Biol Chem* 274: 13139–13146, 1999.
9. Branen L, Hovgaard L, Nitulescu M, Bengtsson E, Nilsson J, and Jovinge S. Inhibition of tumor necrosis factor-alpha reduces atherosclerosis in apolipoprotein E knockout mice. *Arterioscler Thromb Vasc Biol* 24: 2137–2142, 2004.
10. Brice P, Burton H, Edwards CW, Humphries SE, and Aitman TJ. Familial hypercholesterolaemia: a pressing issue for European health care. *Atherosclerosis* 231: 223–226, 2013.
11. Bucciarelli LG, Wendt T, Qu W, Lu Y, Lalla E, Rong LL, Goova MT, Moser B, Kislinger T, Lee DC, Kashyap Y, Stern DM, and Schmidt AM. RAGE blockade stabilizes established atherosclerosis in diabetic apolipoprotein E-null mice. *Circulation* 106: 2827–2835, 2002.
12. Chen Z, Guo L, Zhang Y, Walzem RL, Pendergast JS, Printz RL, Morris LC, Matafonova E, Stien X, Kang L, Coulon D, McGuinness OP, Niswender KD, and Davies SS. Incorporation of therapeutically modified bacteria into gut microbiota inhibits obesity. *J Clin Invest* 124: 3391–3406, 2014.
13. Davies SS, Amarnath V, Montine KS, Bernoud-Hubac N, Boutaud O, Montine TJ, and Roberts LJ, 2nd. Effects of reactive gamma-ketoaldehydes formed by the isoprostane pathway (isoketals) and cyclooxygenase pathway (levuglandins) on proteasome function. *FASEB J* 16: 715–717, 2002.
14. Davies SS, Bodine C, Matafonova E, Pantazides BG, Bernoud-Hubac N, Harrison FE, Olson SJ, Montine TJ, Amarnath V, and Roberts II LJ. Treatment with a gamma-ketoaldehyde scavenger prevents working memory deficits in hApoE4 mice. *J Alzheimers Dis* 27: 49–59, 2011.
15. Davies SS and Roberts LJ, 2nd. F2-isoprostanes as an indicator and risk factor for coronary heart disease. *Free Radic Biol Med* 50: 559–566, 2011.
16. Davies SS, Talati M, Wang X, Mernaugh RL, Amarnath V, Fessel J, Meyrick BO, Sheller J, and Roberts LJ, 2nd. Localization of isoketal adducts in vivo using a single-chain antibody. *Free Radic Biol Med* 36: 1163–1174, 2004.
17. Dawson TC, Kuziel WA, Osahar TA, and Maeda N. Absence of CC chemokine receptor-2 reduces atherosclerosis in apolipoprotein E-deficient mice. *Atherosclerosis* 143: 205–211, 1999.
18. Deane R, Singh I, Sagare AP, Bell RD, Ross NT, LaRue B, Love R, Perry S, Paquette N, Deane RJ, Thiyagarajan M, Zarcone T, Fritz G, Friedman AE, Miller BL, and Zlokovic BV. A multimodal RAGE-specific inhibitor reduces amyloid β–mediated brain disorder in a mouse model of Alzheimer disease. *J Clin Invest* 122: 1377–1392, 2012.
19. Fritz G. RAGE: a single receptor fits multiple ligands. *Trends Biochem Sci* 36: 625–632, 2011.
20. Fuentes E, Rojas A, and Palomo I. Role of multiligand/RAGE axis in platelet activation. *Thromb Res* 133: 308–314, 2014.
21. Fukuda K, Davies SS, Nakajima T, Ong BH, Kupershmidt S, Fessel J, Amarnath V, Anderson ME, Boyden PA, Viswanathan PC, Roberts LJ, 2nd, and Balser JR. Oxidative mediated lipid peroxidation recapitulates proarrhythmic effects on cardiac sodium channels. *Circ Res* 97: 1262–1269, 2005.
22. Galligan JJ, Fritz KS, Backos DS, Shearn CT, Smathers RL, Jiang H, MacLean KN, Reigan PR, and Petersen DR. Oxidative stress-mediated aldehyde adduction of GRP78 in a mouse model of alcoholic liver disease: functional independence of ATPase activity and chaperone function. *Free Radic Biol Med* 73C: 411–420, 2014.
23. Geroldi D, Falcone C, and Emanuele E. Soluble receptor for advanced glycation end products: from disease marker to potential therapeutic target. *Curr Med Chem* 13: 1971–1978, 2006.
24. Gillum MP, Zhang D, Zhang XM, Erion DM, Jamison RA, Choi C, Dong J, Shanabrough M, Duenas HR, Frederick DW, Hsiao JJ, Horvath TL, Lo CM, Tso P, Cline GW, and Shulman GI. N-acylphosphatidylethanolamine, a gut-derived circulating factor induced by fat ingestion, inhibits food intake. *Cell* 135: 813–824, 2008.
25. Grove J, Daly AK, Bassendine MF, and Day CP. Association of a tumor necrosis factor promoter polymorphism with susceptibility to alcoholic steatohepatitis [see comments]. *Hepatology* 26: 143–146, 1997.
26. Gu L, Okada Y, Clinton SK, Gerard C, Sukhova GK, Libby P, and Rollins BJ. Absence of monocyte chemoattractant protein-1 reduces atherosclerosis in low density lipoprotein receptor-deficient mice. *Mol Cell* 2: 275–281, 1998.
27. Guo L, Chen Z, Amarnath V, and Davies SS. Identification of novel bioactive aldehyde-modified phosphatidylethanolamines formed by lipid peroxidation. *Free Radic Biol Med* 53: 1226–1238, 2012.
28. Guo L, Chen Z, Cox BE, Amarnath V, Epand RF, Epand RM, and Davies SS. Phosphatidylethanolamines modified by gamma-ketoaldehyde (gammaKA) induce endoplasmic reticulum stress and endothelial activation. *J Biol Chem* 286: 18170–18180, 2011.
29. Guo L, Gragg SD, Chen Z, Zhang Y, Amarnath V, and Davies SS. Isolevuglandin-modified phosphatidylethanolamine is metabolized by NAPE-hydrolyzing phospholipase D. *J Lipid Res* 54: 3151–3157, 2013.
30. Hansel B, Giral P, Nobecourt E, Chantepie S, Bruckert E, Chapman MJ, and Kontush A. Metabolic syndrome is associated with elevated oxidative stress and dysfunctional dense high-density lipoprotein particles displaying impaired antioxidative activity. *J Clin Endocrinol Metab* 89: 4963–4971, 2004.
31. Harja E, Bu DX, Hudson BI, Chang JS, Shen X, Hallam K, Kalea AZ, Lu Y, Rosario RH, Oruganti S, Nikolla Z, Belov D, Lalla E, Ramasamy R, Yan SF, and Schmidt AM. Vascular and inflammatory stresses mediate atherosclerosis *via* RAGE and its ligands in apoE-/- mice. *J Clin Invest* 118: 183–194, 2008.
32. Haukeland JW, Damas JK, Konopski Z, Loberg EM, Haaland T, Goverud I, Torjesen PA, Birkeland K, Bjoro K, and Aukrust P. Systemic inflammation in nonalcoholic fatty liver disease is characterized by elevated levels of CCL2. *J Hepatol* 44: 1167–1174, 2006.
33. He J, Zhou Y, Xing J, Wang Q, Zhu H, Zhu Y, and Zou MH. Liver kinase B1 is required for thromboxane receptor-dependent nuclear factor-kappaB activation and inflammatory responses. *Arterioscler Thromb Vasc Biol* 33: 1297–1305, 2013.
34. He M, Kubo H, Morimoto K, Fujino N, Suzuki T, Takahasi T, Yamada M, Yamaya M, Maekawa T, Yamamoto Y, and Yamamoto H. Receptor for advanced glycation end products binds to phosphatidylserine and assists in the clearance of apoptotic cells. *EMBO Rep* 12: 358–364, 2011.
35. Hodgkinson CP, Laxton RC, Patel K, and Ye S. Advanced glycation end-product of low density lipoprotein activates the toll-like 4 receptor pathway implications for diabetic

atherosclerosis. *Arterioscler Thromb Vasc Biol* 28: 2275–2281, 2008.
36. Hreggvidsdottir HS, Lundberg AM, Aveberger AC, Klevenvall L, Andersson U, and Harris HE. High mobility group box protein 1 (HMGB1)-partner molecule complexes enhance cytokine production by signaling through the partner molecule receptor. *Mol Med* 18: 224–230, 2012.
37. Hudson BI, Kalea AZ, Del Mar Arriero M, Harja E, Boulanger E, D'Agati V, and Schmidt AM. Interaction of the RAGE cytoplasmic domain with diaphanous-1 is required for ligand-stimulated cellular migration through activation of Rac1 and Cdc42. *J Biol Chem* 283: 34457–34468, 2008.
38. Iannone F and Lapadula G. Obesity and inflammation—targets for OA therapy. *Curr Drug Targets* 11: 586–598, 2010.
39. Koch M, Chitayat S, Dattilo BM, Schiefner A, Diez J, Chazin WJ, and Fritz G. Structural basis for ligand recognition and activation of RAGE. *Structure* 18: 1342–1352, 2010.
40. Kopitz J, Holz FG, Kaemmerer E, and Schutt F. Lipids and lipid peroxidation products in the pathogenesis of age-related macular degeneration. *Biochimie* 86: 825–831, 2004.
41. Lee D, Lee KH, Park H, Kim SH, Jin T, Cho S, Chung JH, Lim S, and Park S. The effect of soluble RAGE on inhibition of angiotensin II-mediated atherosclerosis in apolipoprotein E deficient mice. *PLoS One* 8: e69669, 2013.
42. Li W, Laird JM, Lu L, Roychowdhury S, Nagy LE, Zhou R, Crabb JW, and Salomon RG. Isolevuglandins covalently modify phosphatidylethanolamines in vivo: detection and quantitative analysis of hydroxylactam adducts. *Free Radic Biol Med* 47: 1539–1552, 2009.
43. Libby P, Sukhova G, Lee RT, and Galis ZS. Cytokines regulate vascular functions related to stability of the atherosclerotic plaque. *J Cardiovasc Pharmacol* 25 Suppl 2: S9–S12, 1995.
44. Luo Y, Li SJ, Yang J, Qiu YZ, and Chen FP. HMGB1 induces an inflammatory response in endothelial cells *via* the RAGE-dependent endoplasmic reticulum stress pathway. *Biochem Biophys Res Commun* 438: 732–738, 2013.
45. Manco M. Metabolic syndrome in childhood from impaired carbohydrate metabolism to nonalcoholic fatty liver disease. *J Am Coll Nutr* 30: 295–303, 2011.
46. McGill HC, Jr., McMahan CA, Herderick EE, Zieske AW, Malcom GT, Tracy RE, and Strong JP. Obesity accelerates the progression of coronary atherosclerosis in young men. *Circulation* 105: 2712–2718, 2002.
47. Morris-Rosenfeld S, Blessing E, Preusch MR, Albrecht C, Bierhaus A, Andrassy M, Nawroth PP, Rosenfeld ME, Katus HA, and Bea F. Deletion of bone marrow-derived receptor for advanced glycation end products inhibits atherosclerotic plaque progression. *Eur J Clin Invest* 41: 1164–1171, 2011.
48. Murthi KK, Salomon RG, and Sternlicht H. Levuglandin E2 inhibits mitosis and microtubule assembly. *Prostaglandins* 39: 611–622, 1990.
49. Musiek ES, Brooks JD, Joo M, Brunoldi E, Porta A, Zanoni G, Vidari G, Blackwell TS, Montine TJ, Milne GL, McLaughlin B, and Morrow JD. Electrophilic cyclopentenone neuroprostanes are anti-inflammatory mediators formed from the peroxidation of the omega-3 polyunsaturated fatty acid docosahexaenoic acid. *J Biol Chem* 283: 19927–19935, 2008.
50. Narverud I, Retterstol K, Iversen PO, Halvorsen B, Ueland T, Ulven SM, Ose L, Aukrust P, Veierod MB, and Holven KB. Markers of atherosclerotic development in children with familial hypercholesterolemia: a literature review. *Atherosclerosis* 235: 299–309, 2014.
51. Ohgami N, Nagai R, Ikemoto M, Arai H, Kuniyasu A, Horiuchi S, and Nakayama H. Cd36, a member of the class b scavenger receptor family, as a receptor for advanced glycation end products. *J Biol Chem* 276: 3195–3202, 2001.
52. Parameswaran N and Patial S. Tumor necrosis factor-alpha signaling in macrophages. *Crit Rev Eukaryot Gene Expr* 20: 87–103, 2010.
53. Poliakov E, Brennan ML, Macpherson J, Zhang R, Sha W, Narine L, Salomon RG, and Hazen SL. Isolevuglandins, a novel class of isoprostenoid derivatives, function as integrated sensors of oxidant stress and are generated by myeloperoxidase in vivo. *FASEB J* 17: 2209–2220, 2003.
54. Puntoni M, Sbrana F, Bigazzi F, Minichilli F, Ferdeghini E, and Sampietro T. Myeloperoxidase modulation by LDL apheresis in familial hypercholesterolemia. *Lipids Health Dis* 10: 185, 2011.
55. Rader DJ, Cohen J, and Hobbs HH. Monogenic hypercholesterolemia: new insights in pathogenesis and treatment. *J Clin Invest* 111: 1795–1803, 2003.
56. Robinson SC, Scott KA, and Balkwill FR. Chemokine stimulation of monocyte matrix metalloproteinase-9 requires endogenous TNF-alpha. *Eur J Immunol* 32: 404–412, 2002.
57. Salomon RG, Batyreva E, Kaur K, Sprecher DL, Schreiber MJ, Crabb JW, Penn MS, DiCorletoe AM, Hazen SL, and Podrez EA. Isolevuglandin-protein adducts in humans: products of free radical-induced lipid oxidation through the isoprostane pathway. *Biochim Biophys Acta* 1485: 225–235, 2000.
58. Salomon RG, Jirousek MR, Ghosh S, and Sharma RB. Prostaglandin endoperoxides 21. Covalent binding of levuglandin E2 with proteins. *Prostaglandins* 34: 643–656, 1987.
59. Salomon RG, Subbanagounder G, Singh U, O'Neil J, and Hoff HF. Oxidation of low-density lipoproteins produces levuglandin-protein adducts. *Chem Res Toxicol* 10: 750–759, 1997.
60. Schmidt AM, Hori O, Brett J, Yan SD, Wautier JL, and Stern D. Cellular receptors for advanced glycation end products. Implications for induction of oxidant stress and cellular dysfunction in the pathogenesis of vascular lesions. *Arterioscler Thromb* 14: 1521–1528, 1994.
61. Song F, Hurtado del Pozo C, Rosario R, Zou YS, Ananthakrishnan R, Xu X, Patel PR, Benoit VM, Yan SF, Li H, Friedman RA, Kim JK, Ramasamy R, Ferrante AW, Jr., and Schmidt AM. RAGE regulates the metabolic and inflammatory response to high-fat feeding in mice. *Diabetes* 63: 1948–1965, 2014.
62. Soro-Paavonen A, Watson AM, Li J, Paavonen K, Koitka A, Calkin AC, Barit D, Coughlan MT, Drew BG, Lancaster GI, Thomas M, Forbes JM, Nawroth PP, Bierhaus A, Cooper ME, and Jandeleit-Dahm KA. Receptor for advanced glycation end products (RAGE) deficiency attenuates the development of atherosclerosis in diabetes. *Diabetes* 57: 2461–2469, 2008.
63. Stocker R and Keaney JF, Jr. Role of oxidative modifications in atherosclerosis. *Physiol Rev* 84: 1381–1478, 2004.
64. Sullivan CB, Matafonova E, Roberts LJ, II, Amarnath V, and Davies SS. Isoketals form cytotoxic phosphatidylethanolamine adducts in cells. *J. Lipid Res* 51: 999–1009, 2010.

65. Talati M, Meyrick B, Peebles RS, Jr., Davies SS, Dworski R, Mernaugh R, Mitchell D, Boothby M, Roberts LJ, 2nd, and Sheller JR. Oxidant stress modulates murine allergic airway responses. *Free Radic Biol Med* 40: 1210–1219, 2006.
66. Wang H, Guo J, West X, Bid HK, Lu L, Hong L, Jang GF, Zhang L, Crabb JW, Linetsky MD, and Salomon RG. Detection and biological activities of carboxyethylpyrrole ethanolamine phospholipids: a correlation with age-related macular degeneration. *Chem Res Toxicol* 27: 2015–2022, 2014.
67. Waqar AB, Koike T, Yu Y, Inoue T, Aoki T, Liu E, and Fan J. High-fat diet without excess calories induces metabolic disorders and enhances atherosclerosis in rabbits. *Atherosclerosis* 213: 148–155, 2010.
68. Wendt T, Harja E, Bucciarelli L, Qu W, Lu Y, Rong LL, Jenkins DG, Stein G, Schmidt AM, and Yan SF. RAGE modulates vascular inflammation and atherosclerosis in a murine model of type 2 diabetes. *Atherosclerosis* 185: 70–77, 2006.
69. Xanthis A, Hatzitolios A, Fidani S, Befani C, Giannakoulas G, and Koliakos G. Receptor of advanced glycation end products (RAGE) positively regulates CD36 expression and reactive oxygen species production in human monocytes in diabetes. *Angiology* 60: 772–779, 2009.
70. Xue J, Ray R, Singer D, Bohme D, Burz DS, Rai V, Hoffmann R, and Shekhtman A. The receptor for advanced glycation end products (RAGE) specifically recognizes methylglyoxal-derived AGEs. *Biochemistry* 53: 3327–3335, 2014.
71. Zeng S, Feirt N, Goldstein M, Guarrera J, Ippagunta N, Ekong U, Dun H, Lu Y, Qu W, Schmidt AM, and Emond JC. Blockade of receptor for advanced glycation end product (RAGE) attenuates ischemia and reperfusion injury to the liver in mice. *Hepatology* 39: 422–432, 2004.
72. Zhang H, Tasaka S, Shiraishi Y, Fukunaga K, Yamada W, Seki H, Ogawa Y, Miyamoto K, Nakano Y, Hasegawa N, Miyasho T, Maruyama I, and Ishizaka A. Role of soluble receptor for advanced glycation end products on endotoxin-induced lung injury. *Am J Respir Crit Care Med* 178: 356–362, 2008.
73. Zhang J, Xu X, Rao NV, Argyle B, McCoard L, Rusho WJ, Kennedy TP, Prestwich GD, and Krueger G. Novel sulfated polysaccharides disrupt cathelicidins, inhibit RAGE and reduce cutaneous inflammation in a mouse model of rosacea. *PLoS One* 6: e16658, 2011.
74. Zhang Y, McCluskey K, Fujii K, and Wahl LM. Differential regulation of monocyte matrix metalloproteinase and TIMP-1 production by TNF-alpha, granulocyte-macrophage CSF, and IL-1 beta through prostaglandin-dependent and -independent mechanisms. *J Immunol* 161: 3071–3076, 1998.
75. Zhu C, Solorzano C, Sahar S, Realini N, Fung E, Sassone-Corsi P, and Piomelli D. Proinflammatory stimuli control N-acylphosphatidylethanolamine-specific phospholipase D expression in macrophages. *Mol Pharmacol* 79: 786–792, 2011.

Address correspondence to:
Dr. Sean S. Davies
Department of Pharmacology
Vanderbilt University at Nashville
2220 Pierce Avenue
Room 506A RRB
Nashville, TN 37232-6602

E-mail: sean.davies@vanderbilt.edu

Date of first submission to ARS Central, August 5, 2014; date of final revised submission, December 29, 2014; date of acceptance, February 17, 2015.

Abbreviations Used

AGEs = advanced glycation endproducts
BMDM = bone marrow-derived macrophages
DMEM = Dulbecco's modified Eagle's medium
DMSO = dimethyl sulfoxide
DPPE = 1,2-dipalmitoyl-sn-glycero-3-phosphoethanolamine
EDTA = ethylenediaminetetraacetic acid
ER = endoplasmic reticulum
ETN = ethanolamine
FBS = fetal bovine serum
FH = familial hypercholesterolemia
GPCR = G-protein coupled receptor
HBSS = Hanks' buffered saline solution
HMGB1 = high-mobility group protein box-1
HNE = 4-hydroxynonenal
HPLC = high performance liquid chromatography
IκKβ = Iκ kinase β
IsoLG = isolevuglandins
IsoLG-ETN = isolevuglandin-modified ethanolamine
IsoLG-PE = isolevuglandin-modified phosphatidylethanolamine
LC/MS/MS = HPLC coupled to tandem mass spectrometry
LDL-C = low-density lipoprotein cholesterol
NAPE = N-acyl phosphatidylethanolamine
NAPE-PLD = NAPE-specific phospholipase D
NFκB = nuclear factor kappa B
PBS = phosphate-buffered saline
PE = phosphatidylethanolamine
PLA_2 = phospholipase A_2
qPCR = quantitative real-time PCR
RAGE = receptor for advanced glycation endproducts
sRAGE = soluble form of receptor for advanced glycation endproducts
TNFα = tumor necrosis factor-alpha
TLR = Toll-like receptors